Developmental Biology **240,** 46–60 (2001)
doi:10.1006/dbio.2001.0455, available online at http://www.idealibrary.com on IDEAL®

RARγ and Cdx1 Interactions in Vertebral Patterning

Deborah Allan,*,†,[1] Martin Houle,† Nathalie Bouchard,†,[2] Barbara I. Meyer,‡ Peter Gruss,‡ and David Lohnes*,†,§,[3]

**Division of Experimental Medicine, McGill University, §Department of Molecular Biology, Université de Montréal, †Institut de Recherches Cliniques de Montréal, 110 ave des Pins, ouest, Montréal, Québec, Canada, H2W 1R7; and ‡Department of Molecular Cell Biology, Max Planck Institute of Biophysical Chemistry, Am Fassberg 11, 37077, Gottingen, Germany*

Exogenous retinoic acid (RA) can evoke vertebral homeosis when administered during late gastrulation. These vertebral transformations correlate with alterations of the rostral limit of *Hox* gene expression in the prevertebrae, suggesting that retinoid signaling regulates the combinatorial expression of *Hox* genes dictating vertebral identity. Conversely, loss of certain RA receptors (RARs) results in anterior homeotic transformations principally affecting the cervical region. Despite these observations, the relationship between retinoid signaling, somitic *Hox* expression, and vertebral patterning is poorly understood. The members of the murine *Cdx* family (*Cdx1*, *Cdx2*, and *Cdx4*) are the homologues of *Drosophila caudal* and encode homeobox-containing transcription factors. *Cdx1* homozygous null mutants exhibit anterior homeotic transformations, some of which are reminiscent of those in RARγ null offspring. In *Cdx1* mutants, these transformations occur concomitant with posteriorized prevertebral expression of certain *Hox* genes. *Cdx1* has recently been demonstrated to be a direct RA target, suggesting an indirect means by which retinoid signaling may impact vertebral patterning. To further investigate this relationship, a complete allelic series of *Cdx1-RARγ* mutants was generated and the skeletal phenotype assessed either following normal gestation or after administration of RA. Synergistic interactions between these null alleles were observed in compound mutants, and the full effects of exogenous RA on vertebral morphogenesis required Cdx1. These findings are consistent with a role for RA upstream of *Cdx1* as regards axial patterning. However, exogenous RA attenuated several defects inherent to *Cdx1* null mutants. This finding, together with the increased phenotypic severity of *RARγ–Cdx1* double null mutants relative to single nulls, suggests that these pathways also function in parallel, likely by converging on common targets. © 2001 Academic Press

Key Words: **retinoic acid receptor; *Cdx1*; vertebral patterning; somite; *Hox*; RARE.**

INTRODUCTION

In the mouse, formation of the body axis commences on the sixth day of gestation with the induction of the primitive streak (reviewed in Beddington and Robertson, 1999). Ectodermal cells that ingress through the anterior region of the primitive streak during gastrulation give rise, in part, to paraxial mesoderm, which subsequently segments and differentiates into the laterally paired somites (Wilson and Beddington, 1996; Christ *et al.*, 2000). The sclerotome derivative of somites is the precursor of occipital bones, vertebrae, and ribs. Vertebrae are patterned along the antero-posterior (A-P) axis, which is reflected by their distinctive morphological characteristics, although such differences are often subtle. This patterning relies in large part on the action of the Hox transcription factors (Burke *et al.*, 1995; Gruss and Kessel, 1991; Capecchi, 1997; Sharkey *et al.*, 1997).

The 39 mammalian *Hox* genes are arranged in four groups, *Hoxa–d*, which likely arose by a series of duplication events from a closely related ancestral cluster. *Hox* genes are expressed initially in the posterior embryo at late gastrulation. Subsequently, expression spreads rostrally to reach a distinct anterior boundary in neuroectoderm and mesoderm. Genes located 3′ in each *Hox* cluster are generally expressed earlier and eventually reach a more rostral

[1] Present address: Center for Developmental Biology, UT Southwestern Medical Center, 6000 Harry Hines Blvd., Dallas, Texas 75390-9133.

[2] Present address: Centre de Recherche, Hôtel-Dieu de Québec 9, rue McMahon Québec, Canada, G1R 2J6.

[3] To whom correspondence should be addressed. Fax: (514) 987-5767. E-mail: lohnesd@ircm.qc.ca.

0012-1606/01 $35.00

limit of expression relative to those located more 5′ in a given cluster. This results in the anterior boundaries of *Hox* expression domains being staggered along the length of the axis and, in the case of paraxial mesoderm, these anterior limits usually coincide with somite boundaries.

Based, in part, on the above observations, it was suggested that vertebral A-P identity may be imparted through the expression of a combination of *Hox* genes such that each vertebra is specified by a unique "*Hox* code" (Kessel and Gruss, 1991; Burke *et al.*, 1995; Gruss and Kessel, 1991; Gaunt, 1994). This hypothesis is strongly supported by a multitude of gain- and loss-of-function studies where, in general, anteriorization of *Hox* gene expression results in posterior vertebral homeotic transformation while loss of expression leads to anterior transformations (Maconochie *et al.*, 1999; Kessel and Gruss, 1991; Favier and Dolle, 1999; Capecchi, 1997; Christ *et al.*, 2000). Given this pivotal role in vertebral patterning, *Hox* genes appear to be common targets for a number of factors involved in antero-posterior patterning. Among such factors, targeted disruption of *Fgfr1* (Partanen *et al.*, 1999), *ActRIIB* (Oh and Li, 1997), *Mll* (Yu *et al.*, 1995), or *Cdx1* (Subramanian *et al.*, 1995) leads to abnormal vertebral patterning that is correlated with misexpression of certain *Hox* genes. In mice, administration of exogenous retinoic acid (RA) at late gastrulation (E7.5) also results in posterior vertebral transformations along the entire axis which are correlated with anteriorized limits of prevertebral *Hox* gene expression (Kessel and Gruss, 1991; Conlon and Rossant, 1992; Conlon, 1995). Consistent with this, depletion of embryonic RA by dietary restriction (Gale *et al.*, 1999; Maden *et al.*, 1996) or through targeted disruption of *RALDH2* (an enzyme essential for the generation of most embryonic RA; Niederreither *et al.*, 1999) also has profound effects on rhombomeric *Hox* expression (Niederreither *et al.*, 2000).

The retinoid signal is transduced by two families of nuclear transcription factors, the RARs and the RXRs, each of which is expressed as multiple N-terminal variant isoforms. In the presence of an RAR ligand, RXR-RAR heterodimers activate transcription through retinoic acid response elements (RAREs) in the promoter regions of target genes (Mangelsdorf *et al.*, 1996; Chambon, 1996; Kastner *et al.*, 1996). Consistent with a role for RA in vertebral patterning, a number of RAR null mutant mice exhibit vertebral homeosis, primarily affecting the cervical region (Lohnes *et al.*, 1993, 1994). That the retinoid signal may mediate these effects through *Hox* genes was suggested by the finding that many *Hox* family members respond to excess RA in tissue culture and *in vivo* (Conlon and Rossant, 1992; Kessel and Gruss, 1991; Marshall *et al.*, 1992; Simeone *et al.*, 1990). However, functional RAREs have been identified only for a limited number of such *Hox* genes (Marshall *et al.*, 1994, 1996; Morrison *et al.*, 1996; Studer *et al.*, 1994; Dupé *et al.*, 1997; Huang *et al.*, 1998; Langston and Gudas, 1992; Packer *et al.*, 1998; Frasch *et al.*, 1995; Maconochie *et al.*, 1996; Pöpperl and Featherstone 1993; Zhang *et al.*, 2000). Moreover, to date, none of these RAREs have been shown to be critical for *Hox* function with respect to vertebral patterning. These data suggest that RA may impact on vertebral patterning through indirect regulation of *Hox* transcription.

The *caudal* family of homeobox-containing transcription factors is required for the proper development of the posterior embryo in all species examined to date. The three murine *caudal* homologues, *Cdx1*, *Cdx2*, and *Cdx4*, are expressed in an overlapping expression pattern in the caudal embryo commencing at E7.5 (Gamer and Wright, 1993; Meyer and Gruss, 1993; Beck *et al.*, 1995). *Cdx1* homozygous null mutants and *Cdx2* heterozygous offspring exhibit anterior homeotic transformations in the cervical and thoracic regions of the vertebral column which occur concomitant with posterior shifts in expression of some *Hox* genes, at least in $Cdx1^{-/-}$ offspring (Subramanian *et al.*, 1995; Chawengsaksophak *et al.*, 1997). Similar homeotic transformations are also found (at a low incidence) in *RARγ* null offspring, demonstrating functional convergence between these transcription factors (Lohnes *et al.*, 1993). A direct relationship between these two pathways is further supported by the finding that *Cdx1* is a direct RAR target gene, suggesting that *Cdx1* may serve as an intermediary for *Hox* regulation and vertebral specification elicited by the retinoid signal (Houle *et al.*, 2000). In the present study, we further investigated this relationship by generation and analysis of *Cdx1–RARγ* compound mutant mice. We demonstrate that *Cdx1* is required for some of the effects of exogenous RA on the axial skeleton, and that it acts both downstream of, and parallel to, retinoid signaling during vertebral patterning.

MATERIALS AND METHODS

Embryos and RA Treatment

The *RARγ* and *Cdx1* null mice used in this study have been previously described (Lohnes *et al.*, 1993; Subramanian *et al.*, 1995). *Cdx1–RARγ* double heterozygotes as well as $Cdx1^{-/-}$--$RAR\gamma^{+/-}$ progeny were generated and used in subsequent crosses to derive all possible combinations of offspring. Mice were mated overnight and females examined the following morning for the presence of a vaginal plug; noon of the day of plug was considered as E0.5. Pregnant females were dosed by oral gavage with all-*trans* RA dissolved in DMSO and subsequently diluted in corn oil to a final delivery of 10 mg/kg at E7.5 or 100 mg/kg at E8.5, E9.5, or E10.5, and either allowed to carry to term or sacrificed 48 h postgavage (treatment at E7.5 only). In the latter case, embryos were dissected in phosphate buffered saline (PBS), fixed overnight in 4% paraformaldehyde, dehydrated through a methanol series and stored at −20°C in 100% methanol. Genotype was determined by PCR using DNA isolated from either yolk sac or skin as described previously for RARγ (Iulianella and Lohnes, 1997). For *Cdx1*, primers specific for the *Cdx1* locus (5′-CCCCACAGGTAAAGATCTGG-3′ and 5′-CCCCAAAGGCAGCAGCAGGG-3′) which flank the *Neo* integration site (Subramanian *et al.*, 1995) were used to amplify an approximately 330-bp product specific for the wild-type allele. The primer 5′-GGCCGGAGAACCTGCGTGCAATCC-3′, located in the 5′ coding region of the

Neo gene, was employed with the second oligonucleotide to amplify an approximately 600-bp product specific for the disrupted allele. For some *in situ* hybridization analysis, wild-type controls were derived either from the above matings or from CD-1 intercrosses; no overt differences in gene expression were observed between these two control backgrounds.

In Situ Hybridization Analysis

Embryos were pooled by stage (judged by somite number), genotype, and RA treatment and rehydrated through a methanol series. The *Hoxd3* and *Hoxd4* cDNAs (Condie and Capecchi 1993; Folberg *et al.*, 1997) were used to generate digoxigenin-labeled riboprobes and whole-mount *in situ* hybridizations performed as described (Iulianella *et al.*, 1999). Samples to be compared were processed in parallel under identical conditions to control for interexperimental variation in signal strength. Following signal development, embryos were cleared and photographed under a dissecting microscope.

Whole-mount skeletal preparations. Fetuses were skinned, eviscerated, and dehydrated in 100% ethanol. Carcasses were then stained overnight with 0.03% Alcian blue (Sigma) in 80% ethanol: 20% glacial acetic acid (v/v) to reveal cartilaginous elements. Specimens were then dehydrated in 100% ethanol, cleared in 2% aqueous potassium hydroxide for 6 h, and stained overnight with 0.1% Alizarin Red S (Sigma) to detect ossified structures. Clearing was subsequently effected by several changes of 20% glycerol in 1% potassium hydroxide followed by 50% glycerol:50% ethanol (v/v) for 2–3 weeks. Specimens were scored under a dissecting microscope and photographed.

RESULTS

All $Cdx1^{-/-}$ mice were viable and fertile, as expected, and the additional loss of one allele of $RAR\gamma$ had no apparent effect on the reproductive capacity or longevity of $Cdx1^{-/-}$–$RAR\gamma^{+/-}$ compound mutants. Analysis of 55 newborn mice from $Cdx1^{-/-}RAR\gamma^{+/-}$ intercrosses revealed 13 (24%) $Cdx1^{-/-}$, 26 (47%) $Cdx1^{-/-}RAR\gamma^{+/-}$, and 16 (29%) $Cdx1^{-/-}RAR\gamma^{-/-}$ offspring, demonstrating that $Cdx1/RAR\gamma$ double null mutants survive to term. The vertebral homeotic transformations and malformations observed in the various $Cdx1$–$RAR\gamma$ mutants are summarized in Table 1 and are described below.

In the mouse, the vertebral column is normally composed of 7 cervical (C1–C7), 13 thoracic (T1–T13), 6 lumbar (L1–L6), 3 or 4 sacral (S1–S4), and 31 caudal vertebrae. The first cervical vertebra (C1, or atlas) has thick neural arches, lacks a true vertebral body, and possesses a ventrally located tubercle, the anterior arch of the atlas (AAA). The neural arches of C2 are not as broad as those of C1, but are thicker than those of more posterior cervical vertebrae. C2 also possesses two vertebral bodies, the second of which (the dens axis) is composed of material derived from C1, and is located directly anterior to the vertebral body of the axis. Vertebrae C3–C5 are virtually identical to one another, all possessing transverse foramen and articular processes that extend in the plane of the body. C6 is distinguished by the ventrally protruding anterior tuberculi, whereas C7 resembles C3–C5 but lacks transverse foramen. The thoracic vertebrae are characterized by the presence of ribs, the first seven of which (T1–T7) attach to the sternum. The second thoracic vertebra is further distinguished by a large dorsal spinous process.

Vertebral Defects in Cdx1 and RARγ Null Mutants

In contrast to previous studies (Subramanian *et al.*, 1995), anterior transformations and vertebral malformations were found in $Cdx1^{+/-}$ offspring (Table 1). C2 often exhibited partial characteristics of C1, including the presence of an ectopic AAA-like structure and/or thicker neural arches (Fig. 1D). Caudal extension of the basioccipital, or the fusion of this bone to the AAA, was observed in 31% of heterozygous offspring (Fig. 1E). Malformation of the neural arches of C1 and C2 and fusions of C2–C3 were also detected (Figs. 1F). More caudal vertebrae typically affected in *Cdx1* null mutants (see below) were normal in the heterozygotes, suggesting that the anterior-most vertebral elements are particularly sensitive to *Cdx1* gene dosage.

The skeletal phenotype of $Cdx1^{-/-}$ mice agreed with prior work (Subramanian *et al.*, 1995), although slightly higher frequencies and/or penetrance of defects were noted in the present study (Table 1). Briefly, all *Cdx1* null mutants exhibited close apposition or fusion of C1 to the basioccipital bone, a reduction of the C1 neural arches and loss of the AAA (Figs. 2B and 3). Concomitantly, a rostral shift in the identities of C2, C3, C6, and C7 by one vertebra was observed, as evidenced by altered morphological features. Most $Cdx1^{-/-}$ skeletons exhibited ribs on the eighth vertebra (presumptive T1) which were, however, either fused to the ribs of vertebra 9 or only partially formed (denoted incomplete ribs in Table 1). Thirty eight percent of the skeletons exhibited a T1 to C7 phenotype. However, the number of rib-bearing or lumbar vertebrae was usually reduced by one (i.e., C8/T12/L6 or C8/T13/L5 vertebral patterns in Table 1), and hence the number of presacral vertebrae did not differ from controls. Finally, the spinous process characteristic of vertebra 9 was found on vertebra 9 and/or 10 in approximately half of the $Cdx1^{-/-}$ skeletons. As previously discussed (Subramanian *et al.*, 1995), these data are consistent with anterior homeotic transformation of vertebrae C1 through T8 elicited by *Cdx1* disruption.

The homeotic transformations and vertebral malformations observed in $RAR\gamma$ mutants have been previously described (Lohnes *et al.*, 1993) and are consistent with the present study. These defects included caudal extension of the basioccipital bone and fusion of this bone to the AAA, and partial C2-to-C1 anterior transformation, all of which occurred at a low penetrance (Table 1 and data not shown).

Compound Mutants

$Cdx1^{+/-}$–$RAR\gamma^{+/-}$ offspring. The incidence of several vertebral defects was increased in $Cdx1^{+/-}$--$RAR\gamma^{+/-}$ offspring relative to either single heterozygote (Table 1). These

TABLE 1
Vertebral Phenotypes of Compound *Cdx1–RARγ* Mutants

	Genotype								
Phenotype	WT $n = 23$ (%)	RARγ$^{+/-}$ $n = 38$ (%)	RARγ$^{-/-}$ $n = 27$ (%)	Cdx1$^{+/-}$ $n = 38$ (%)	Cdx1$^{-/-}$ $n = 29$ (%)	Cdx1$^{+/-}$γ$^{+/-}$ $n = 42$ (%)	Cdx1$^{+/-}$γ$^{-/-}$ $n = 15$ (%)	Cdx1$^{-/-}$γ$^{+/-}$ $n = 32$ (%)	Cdx1$^{-/-}$γ$^{-/-}$ $n = 20$ (%)
Basioccipital									
Fusion to AAA	—	—	1 (4)	5 (13)	29 (100)	3 (7)	6 (40)	32 (100)	20 (100)
Caudal Extension	—	—	2 (7)	7 (18)	—	16 (38)	3 (20)	—	—
Vertebrae 1									
Fusion to occipitals	—	—	—	—	29 (100)	—	—	32 (100)	20 (100)
Malformed NA[c]	—	—	—	6 (16)	—	4 (10)	9 (60)	1 (3)[a]	—
Vertebrae 2									
Complete C1 identity	—	—	—	—	29 (100)	—	—	32 (100)	20 (100)
Partial C1 identity									
AAA	—	—	3 (11)	17 (44)	—	21 (50)	13 (87)	—	—
Thick NA	—	3 (8)[a]	11 (41)	17 (44)	—	34 (81)	5 (33)	—	—
Malformed NA	—	—	—	16 (42)	—	11 (26)	8 (53)	4 (13)	1 (5)[a]
Fusion to V3	—	—	—	10 (26)	4 (14)	10 (24)	5 (34)	2 (6)	—
Vertebrae 3									
Complete C2 identity	—	—	—	—	29 (100)	—	—	32 (100)	20 (100)
Thick NA	—	—	—	—	—	2 (5)	8 (53)	—	—
Vertebrae 6									
No TA	—	—	—	1 (4)[a]	29 (100)	5 (12)[a]	2 (13)[a]	31 (97)[b]	20 (100)
Vertebrae 7									
TA	—	—	—	—	28 (97)[b]	4 (10)[a]	2 (13)[a]	32 (100)	20 (100)
Rib	—	1 (3)[a]	—	—	—	—	—	—	—
Vertebrae 8									
C7 identity	—	—	—	—	11 (38)	—	—	16 (50)	16 (80)
Incomplete rib	—	—	—	—	18 (62)	—	—	16 (50)	4 (20)[b]
Spinous process on:									
V10	—	—	—	—	6 (27)	—	1 (7)	7 (22)	9 (45)
V8 and V9	—	1 (3)	1 (4)	—	—	—	—	—	—
V9 and V10	—	1 (3)	2 (7)	—	6 (27)	—	4 (27)	15 (47)	8 (40)
Cervical vertebrae:									
6	—	1 (3)[a]	—	—	—	—	—	—	—
8	—	—	—	—	11 (38)	—	—	15 (47)	16 (80)
Ribs									
12	—	—	—	—	13 (45)	—	—	14 (44)	8 (40)
14	1 (4)[b]	4 (11)[a]	15 (56)	—	2 (7)	—	9 (60)	4 (13)	3 (15)[a]
Sternal Ribs									
6	—	—	—	—	6 (21)[a]	—	—	1 (3)[a]	—
8	4 (17)[a]	6 (16)	21 (78)	9 (24)	4 (14)[a]	16 (38)	14 (93)	6 (19)[a]	—
Lumbar vertebrae:									
5	4 (17)	4 (11)	15 (56)	4 (11)	6 (21)	6 (14)	9 (60)	6 (19)	15 (75)
Vertebral pattern[d]									
C6/T14/L6	—	1 (3)	—	—	—	—	—	—	—
C7/T12/L6	—	—	—	—	—	—	—	—	—
C7/T13/L5	3 (13)	2 (5)	—	4 (11)	2 (7)	6 (14)	—	1 (13)	—
C7/T13/L6	19 (83)	32 (84)	12 (44)	34 (89)	14 (48)	36 (86)	6 (40)	14 (44)	2 (10)
C7/T14/L5	1 (4)	2 (5)	15 (56)	—	2 (7)	—	9 (60)	4 (13)	6 (30)
C7/T14/L6	—	1 (3)	—	—	—	—	—	1 (3)	—
C8/T12/L5	—	—	—	—	—	—	—	1 (3)	—
C8/T12/L6	—	—	—	—	10 (34)	—	—	11 (34)	5 (25)
C8/T13/L5	—	—	—	—	2 (7)	—	—	3 (9)	13 (65)
C8/T13/L6	—	—	—	—	1 (3)	—	—	1 (3)	—

[a] All unilateral.
[b] All bilateral.
[c] Includes fusions.
[d] The total may exceed the number of samples noted as some offspring exhibited two different (unilateral) vertebral patterns.

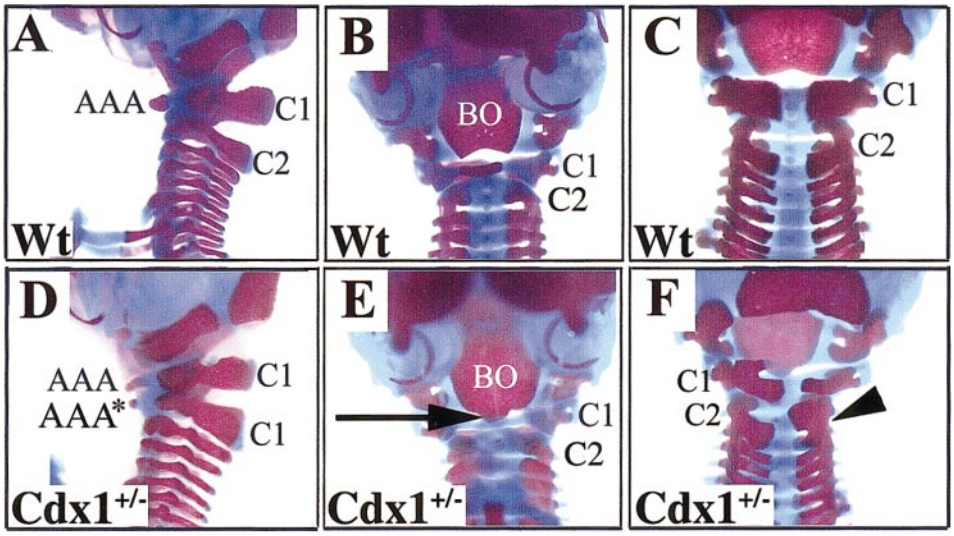

FIG. 1. *Cdx1* heterozygote skeletal phenotypes. Whole-mount skeletal preparations from (A–C) wild-type and (D–F) *Cdx1* heterozygous offspring. (A, D) Lateral view of cervical region of a wild-type (A) and a $Cdx^{+/-}$ specimen (B). AAA* in (D) denotes an ectopic anterior arch of the atlas in the heterozygous sample. (B, E) Ventral view of the base of the skull of a wild-type (B) and a *Cdx1* heterozygote (E). The caudal extension of the basioccipital bone in the heterozygote is indicated by an arrow in (E). (C, F) Dorsal view of the cervical region of a control (C) and a *Cdx* heterozygote (F). Note the malformations and fusions of the neural arches in the heterozygous specimen, indicated by the arrowhead in (F). Abbreviations: AAA, anterior arch of the atlas; BO, basioccipital; C, cervical vertebra.

included caudal extension of the basioccipital bone and partial C2–C1 transformation, as evidenced by a thickening of the C2 neural arches. Anterior transformations of C6-to-C5 and C7-to-C6 were also increased, as determined by the loss or gain of anterior tuberculi, respectively (Table 1 and Figs. 2C–2E).

Cdx1*$^{+/-}$*–RARγ*$^{-/-}$*offspring. As described in Table 1, $Cdx1^{+/-}$–$RAR\gamma^{-/-}$ offspring were more affected than double heterozygotes or *RARγ* null mutants. $Cdx1^{+/-}$--$RAR\gamma^{-/-}$ skeletons exhibited an increased incidence of fusion of the basioccipital bone to the AAA (Fig. 2F). This fusion occured significantly more frequently than would be expected from an additive effect ($P < 0.025$). The majority of $Cdx1^{+/-}RAR\gamma^{-/-}$ skeletons also exhibited malformed neural arches of C1 through C3, which were also often fused to the neural arches of the adjoining vertebral element (Fig. 2F). An ectopic AAA on C2, frequently fused to the normal AAA, was also observed in most of these specimens (Fig. 2F), and C3 frequently exhibited thickened neural arches indicative of a partial transformation to a C2 identity. The above defects were rarely seen in the double heterozygotes or in RARγ single null mutants, further demonstrating that *Cdx1* and *RARγ* act synergistically in vertebral patterning.

Cdx1*$^{-/-}$*–RARγ*$^{+/-}$*offspring. These offspring presented vertebral phenotypes essentially identical to $Cdx1^{-/-}$ samples with the exception of a low incidence of fusions involving C1 through C3 (Fig. 2G, Table 1, and data not shown).

Cdx1/RARγ double null mutants. In marked contrast to *Cdx1* null offspring or *Cdx1/RARγ* compound mutants, all of which exhibited readily identifiable vertebral defects, the cervical region of most double null mutants appeared superficially normal (Figs. 2H and 3). However, upon closer examination, this was found to be due to an essentially complete fusion between C1 and the exoccipitals, relative to $Cdx1^{-/-}$ mice (Fig. 3); this could be interpreted as a more expressive anterior transformation of C1 into an occipital identity. Anterior transformations continued throughout the cervical region with the C2 through C7 exhibiting anterior shifts in morphological identities in all double mutants, as well as an increased incidence of T1-to-C7 transformation (observed in 38% of all $Cdx1^{-/-}$ skeletons) present in the majority of these specimens (Fig. 3). The appearance of this latter transformation was not likely due to the insertion of a cervical element, as all affected $Cdx1^{-/-}RAR\gamma^{-/-}$ skeletons possessed 12 thoracic or 5 lumbar vertebrae, thus maintaining the number of presacral vertebrae at 26. The majority of double null offspring with T1-to-C7 transformations exhibited vertebral patterns of C8/T13/L5 (Table 1; note that the use of C8 designates the occipital-C1 fusion as C1, hence the T1-to-C7 transformation results in the assignment of 8 cervical vertebrae). This is in contrast to the majority of $Cdx1^{-/-}$ skeletons with the same T1–C7 transformation, which had vertebral patterns of C8/T12/L6. Therefore, the loss of *RARγ* from the *Cdx1* null background also appears to mediate L1 to thoracic homeosis, suggesting convergent roles for these gene products in patterning more caudal vertebrae; such functions are masked in either single null background. With the exception of C2-to-C1 homeosis, these transformations have

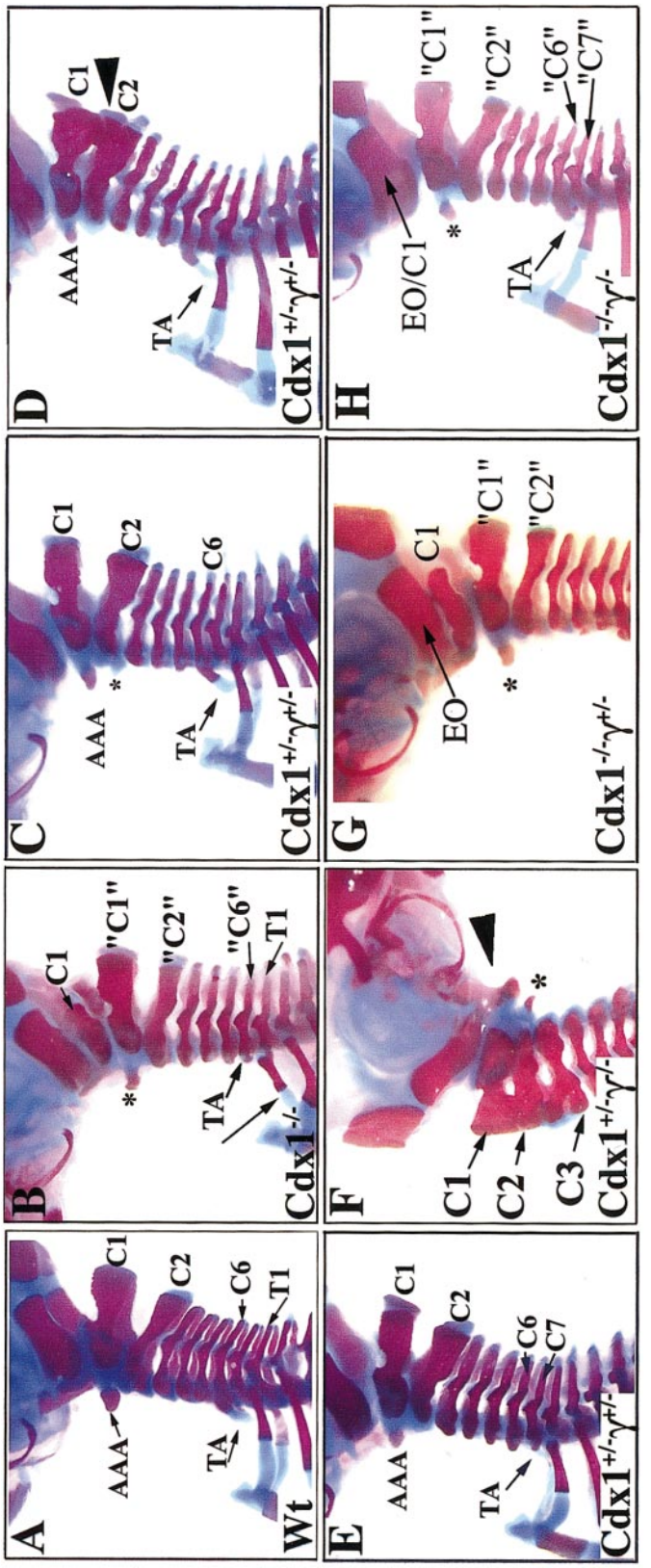

FIG. 2. Skeletal phenotypes of *Cdx1/RARγ* compound mutants. (A, B) Lateral views of the cervical region of a wild-type skeleton (A) and of a Cdx1 null mutant (B). Note the loss of the anterior arch of the atlas in the mutant, and the malformation and malposition of C1. Note also the anterior transformation of C2, C3, and C7 to more anterior elements denoted by "C1," "C2," and "C6," respectively; transformations are evidenced by an ectopic anterior arch (*), wider neural arches on "C2" and a tuberculum anterior on "C6." The arrow in (B) indicates a partial rib associated with the presumptive T1 which does not reach the sternum. (C–E) *Cdx1–RARγ* double heterozygotes. Note the partial C2-to-C1 transformation evidenced by an ectopic anterior arch of the atlas (* in C), malformations of C1 and C2 (arrowhead in D) and C7-to-C6 transformation evidenced by a tuberculum anterior (TA) on C7 in (E). (F) A $Cdx1^{+/-}RARγ^{-/-}$ specimen exhibiting malformation of C1 through C3 (arrows), caudal extension, and fusion of the basioccipital bone with the anterior arch of the atlas (arrowhead), and an ectopic anterior arch (*). (G) Represents a typical $Cdx1^{-/-}RARγ^{+/-}$ sample, with a C1 partially fused to the exoccipital (EO), and C2 and C3 anteriorly transformed (indicated by "C1" and "C2"; note also the ectopic anterior arch denoted by *). (H) A double null mutant. Note the normal appearance of the cervical region, resulting from an anterior shift in vertebral identity of C1 through T1, (indicated by "C1" through "C7") and a more complete fusion of C1 with the exoccipital bone (EO/C1). Abbreviations: EO, exoccipital; AAA, anterior arch of the atlas. TA, tuberculum anterior. C, cervical; T, thoracic; EO/C1, complete fusion of the exoccipital bone with C1. *, Ectopic anterior arch of the atlas; Quotation marks indicate presumptive anterior transformations.

never been observed at a significant frequency in *RARγ*$^{-/-}$ offspring, demonstrating that loss of *RARγ* increases the incidence of homeosis in the *Cdx1*$^{-/-}$ background in a dose-dependent manner (Table 1).

The loss of the remaining *Cdx1* allele from the *Cdx1*$^{+/-}$ *RARγ*$^{-/-}$ background was also striking in that it appeared to correct the vertebral fusions and other nonhomeotic defects observed in most *Cdx1*$^{+/-}$*RARγ*$^{-/-}$ offspring, superficially leading to the appearance of a normal cervical skeleton. This suggests that these neural arch fusions, which have been described in a number of *RAR*, *Hox*, and other mutants, may be indicative of an intermediate state of homeosis which is resolved in the double null offspring.

Hox Gene Expression in Cdx1–RARγ Null Mutants

Both RARs and *Cdx1* have been implicated in *Hox* gene regulation. Consistent with this, both RA excess and *Cdx1* loss alter the anterior expression boundaries of certain *Hox* genes concomitant with vertebral homeosis (Subramanian *et al.*, 1995; Kessel and Gruss, 1991). To investigate altered *Hox* expression as the basis for the synergy observed between *RARγ*$^{-/-}$ and *Cdx1*, the expression patterns of *Hoxd3* and *Hoxd4* were examined by *in situ* hybridization in wild-type, *Cdx1*$^{-/-}$, and *Cdx1*$^{-/-}$–RAR$\gamma^{-/-}$ E9.5 embryos. The anterior boundary of *Hoxd3* in the paraxial mesoderm normally lies between somites 4 and 5. *Hoxd3* mutants exhibit fusion of C1 to the occipitals, and partial transformation of C2 to C1 (Condie and Capecchi, 1993), and its expression is shifted posteriorly in *Cdx1*$^{-/-}$ offspring (Subramanian *et al.*, 1995). Thus, *Hoxd3* is an attractive candidate for the synergy between RA and Cdx1 signaling affecting C1-basioccipital fusion. However, to date, we have not detected further reduction of *Hoxd3* expression in *RARγ–Cdx1* double null mutants.

At E9.5, *Hoxd4* has an anterior limit of strong expression in somite 6, with weaker expression in somite 5 (Folberg *et al.*, 1997). *Hoxd4* null embryos exhibit certain of the homeotic transformations that are observed in *Cdx1*$^{+/-}$ and *RARγ*$^{-/-}$ skeletons, notably caudal extension of the basioccipital bone and C2-to-C1 anterior transformation (Horan *et al.*, 1995a,b; Lohnes *et al.*, 1993). Moreover, *RARγ* and *Hoxd4* null mutations also exhibit synergy as regards fusion of the basioccipital bone and the AAA and partial C2-to-C1 transformation (Folberg *et al.*, 1999), suggesting that altered expression of *Hoxd4* may underlie some of the synergism seen between *Cdx1* and *RARγ* null alleles. However, *Hoxd4* expression was not appreciably altered in *Cdx1* single or *Cdx1–RARγ* double null embryos relative to wild-type controls (data not shown).

Exogenous RA Attenuates Vertebral Homeosis in Cdx1 Null Mutants

Ectopic expression of *Cdx1* during development can evoke vertebral and neural tube defects (Charité *et al.*, 1998; Isaacs *et al.*, 1998; Pownall *et al.*, 1996) reminiscent of the effects of excess RA. These observations suggested that some of the teratogenic effects of RA may occur through misexpression of *Cdx1*. To investigate this, pregnant females from *Cdx1*$^{+/-}$ intercrosses were treated with RA at E7.5–E10.5, and surviving fetuses assessed for skeletal defects. As regards the outcome of treatment at later stages, all of the resultant offspring exhibited identical frequency and severity of axial truncation (RA on E8.5) or limb defects (RA on E9.5–E10.5) irrespective of genotype (data not shown). Cdx1 therefore appears to be dispensable for evoking these particular teratogenic outcomes.

RA treatment at E7.5 results in homeotic transformations along the entire vertebral axis (Kessel and Gruss, 1991); similar abnormalities were observed in wild-type offspring in this study (Table 2). These included fusion of the basioccipital bone to the AAA or the dens axis and induction of a "proatlas" (Fig. 4B). This latter structure derives from the 5th and 6th somites, which normally contribute to the basioccipital bone and the tip of the dens axis. Induction of a proatlas is interpreted as a posterior transformation based on its similarity to C1. It is unlikely that this vertebral pattern is due to an anterior transformation of C2 to C1 based both on morphological criteria (Kessel and Gruss, 1991) and by the fact that RA treatment generally results in posterior vertebral homeosis in the cervical region (Conlon, 1995; Kessel and Gruss, 1991). Consistent with this, a vertebral body was present in 16% of the C1 vertebrae, indicating transformation to a C2 identity. However, these affected vertebrae retained an AAA and neural arches typical of C1 and therefore the transformation was incomplete. The second cervical vertebra exhibited a partial or complete transformation to C3 in approximately half of the samples, and posteriorization of C5 and C6 occurred in 32% of the offspring, as determined by the presence or absence of anterior tuberculi, respectively. These transformations were often accompanied by the loss of one or two cervical vertebrae, thereby reducing the total number (not including the proatlas) to five or six elements. This loss did not appear to be compensated by the gain of more caudal vertebrae as the number of presacral vertebrae was also reduced by one or two units (Table 2). The previously described resistance of *RARγ* mutant embryos to RA-induced transformations and malformations at E7.5 (Iulianella and Lohnes, 1997) was observed in the present study. This included a reduction in the incidence and penetrance of proatlas formation and posterior transformation of C1 to C2 or C2 to C3 (Table 2).

Excess RA at E7.5 had profound effects on the incidence of vertebral homeosis normally seen in *Cdx1* heterozygous and null mutants (Table 2). The frequency of defects involving the basioccipital bone (caudal extension and fusion with the AAA) was greatly reduced following treatment. RA also abrogated defects inherent to vertebra 1, which was rarely fused to the basioccipital and often possessed a complete AAA following treatment (Fig. 4E). This "rescue" effect was also seen in more posterior elements, with treatment greatly reducing the incidence of anterior transformation of

TABLE 2

Vertebral Phenotypes of Compound *Cdx1–RARγ* Mutant Mice Treated with RA at E7.5

	Genotype								
Phenotype	WT $n = 19$ (%)	RARγ$^{+/-}$ $n = 9$ (%)	RARγ$^{-/-}$ $n = 8$ (%)	Cdx1$^{+/-}$ $n = 7$ (%)	Cdx1$^{-/-}$ $n = 7$ (%)	Cdx1$^{-/-}$γ$^{+/-}$ $n = 10$ (%)	Cdx1$^{+/-}$γ$^{-/-}$ $n = 5$ (%)	Cdx1$^{-/-}$γ$^{+/-}$ $n = 3$ (%)	Cdx1$^{-/-}$γ$^{-/-}$ $n = 9$ (%)
Basioccipital									
Fusion to: AAA	1 (5)	—	—	1 (14)	—	—	3 (60)	3 (100)	9 (100)
Dens	2 (11)	—	—	—	—	—	1 (20)	—	—
Caudal extension	1 (5)	—	—	2 (29)	1 (14)	—	—	—	—
Proatlas									
Evidence for	—	1 (11)[b]	2 (25)[a]	3 (43)	2 (29)	—	—	—	—
Complete	6 (32)[b]	1 (11)[b]	—	—	—	—	—	—	—
Vertebra 1									
Fusion to occipitals	—	—	—	—	—	—	—	2 (67)[b]	5 (56)
Partial C2 identity	4 (21)	1 (11)	1 (13)[a]	1 (14)[b]	1 (14)[b]	—	—	—	—
Fusion to V2	4 (21)	2 (22)[a]	—	2 (29)	4 (57)	—	2 (40)	1 (33)	8 (89)
Malformed NA[c]	3 (16)	4 (44)	2 (25)[a]	2 (29)	3 (43)[b]	1 (10)[a]	3 (60)	—	—
Vertebra 2									
Complete C1 identity	—	—	—	—	—	—	—	3 (100)	8 (89)
Partial C1 identity									
AAA	—	—	—	1 (14)	3 (43)[i]	2 (20)	4 (80)	—	1 (11)
Thick NA	—	—	—	1 (14)[b]	3 (43)[b]	1 (10)[b]	1 (20)[b]	—	1 (11)[b]
Complete C3 identity	3 (16)	—	—	—	—	—	—	—	—
Partial C3 identity	6 (32)	—	—	—	1 (14)[b]	—	—	—	—
Malformed NA[c]	3 (16)	2 (22)	—	4 (57)	3 (43)	1 (10)[b]	3 (60)[b]	1 (33)[b]	—
Fusion to V3	—	—	—	—	1 (14)[a]	—	2 (40)	—	3 (33)
Vertebra 3									
Complete C2 identity	—	—	—	—	—	—	—	3 (100)	8 (89)
Partial C2 identity									
Thick NA	—	—	—	—	—	—	—	—	1 (11)[b]
Malformed NA[c]	—	—	—	—	—	—	3 (60)	—	—
Vertebra 5									
TA	6 (32)	3 (33)[b]	4 (50)	4 (57)	2 (29)[a]	—	—	—	—
Vertebra 6									
C5 identity	—	—	—	—	—	—	3 (60)	2 (67)[b]	5 (56)[b]
C7 identity	6 (32)	3 (33)[b]	4 (50)	3 (43)[b]	2 (29)[a]	—	—	—	—
Rib	1 (5)[b]	—	—	1 (14)[b]	—	—	—	—	—
Vertebra 7									
TA	—	—	—	—	—	—	3 (60)	2 (67)[b]	5 (56)[b]
Rib: Incomplete	2 (11)[b]	—	—	1 (14)[b]	2 (29)[a]	2 (20)	1 (20)[a]	—	—
Complete	7 (37)[b]	3 (33)[b]	4 (50)[b]	4 (57)[b]	4 (57)[b]	1 (10)[a]	—	—	—
Vertebra 8									
C7 identity	—	—	—	—	—	—	1 (20)[a]	1 (33)[a]	3 (33)[b]
Incomplete rib	1 (5)[b]	—	—	—	—	—	1 (20)[a]	2 (67)	2 (22)
Spinous process on:									
V7	1 (5)	—	—	1 (14)	—	—	—	—	—
V8	6 (32)	3 (33)	4 (50)	4 (57)	5 (71)	2 (20)	—	—	—
V10	—	—	—	—	—	—	—	—	3 (33)
V8 and V9	2 (11)	—	—	—	1 (14)	—	—	—	—
V9 and V10	—	—	—	—	—	1 (10)	3 (60)	1 (33)	1 (11)
Cervical Vertebrae									
5	1 (5)[b]	—	—	1 (14)[b]	—	—	—	—	—
6	8 (42)[b]	3 (33)[b]	4 (50)[b]	4 (57)[b]	6 (86)	2 (20)	—	—	—
8	—	—	—	—	—	—	1 (20)[a]	1 (33)[a]	3 (33)[b]
Sternal ribs									
6	2 (11)	—	1 (13)[a]	—	—	—	—	—	—
8	3 (16)	3 (33)[a]	5 (63)	1 (14)[b]	—	7 (70)	3 (60)	—	1 (11)[a]
Total Ribs									
12	1 (5)[b]	—	—	1 (14)[b]	1 (14)[b]	—	—	1 (33)[a]	2 (22)[b]
14	6 (32)	1 (11)[a]	4 (50)	1 (14)[b]	—	7 (70)	4 (80)	—	1 (11)[b]
Lumbar vertebrae									
5	11 (53)	3 (33)	4 (50)	3 (43)[b]	4 (57)	5 (50)	1 (20)[a]	1 (33)[b]	6 (67)[b]
Vertebral pattern[d]									
C5/T13/L5	—	—	—	1 (14)	—	—	—	—	—
C5/T14/L5	1 (5)	—	—	—	—	—	—	—	—
C6/T13/L5	3 (16)	2 (22)	—	2 (29)	3 (43)	—	—	—	—
C6/T13/L6	3 (16)	1 (11)	2 (25)	2 (29)	3 (43)	2 (20)	—	—	—
C6/T14/L5	2 (11)	—	3 (38)	—	—	1 (10)	1 (20)	—	—
C6/T14/L6	—	—	1 (13)	—	—	—	—	—	—
C7/T12/L5	1 (5)	—	—	—	—	—	—	—	—
C7/T12/L6	1 (5)	—	—	1 (14)	1 (14)	—	—	—	2 (22)
C7/T13/L5	1 (5)	—	—	—	1 (14)	1 (10)	1 (20)	1 (33)	2 (22)
C7/T13/L6	5 (26)	5 (56)	3 (38)	—	—	1 (10)	1 (20)	1 (33)	1 (11)
C7/T14/L5	3 (16)	1 (11)	1 (13)	—	—	3 (30)	3 (60)	—	1 (11)
C7/T14/L6	—	—	—	1 (14)	—	3 (30)	—	—	—
C8/T13/L5	—	—	—	—	—	—	1 (20)	1 (33)	3 (33)

[a] Unilateral.

[b] Bilateral.

[c] Includes fusions of neural arches.

[d] Not including proatlas.

[e] The total may exceed the number of samples noted as some offspring exhibited two different (unilateral) vertebral patterns.

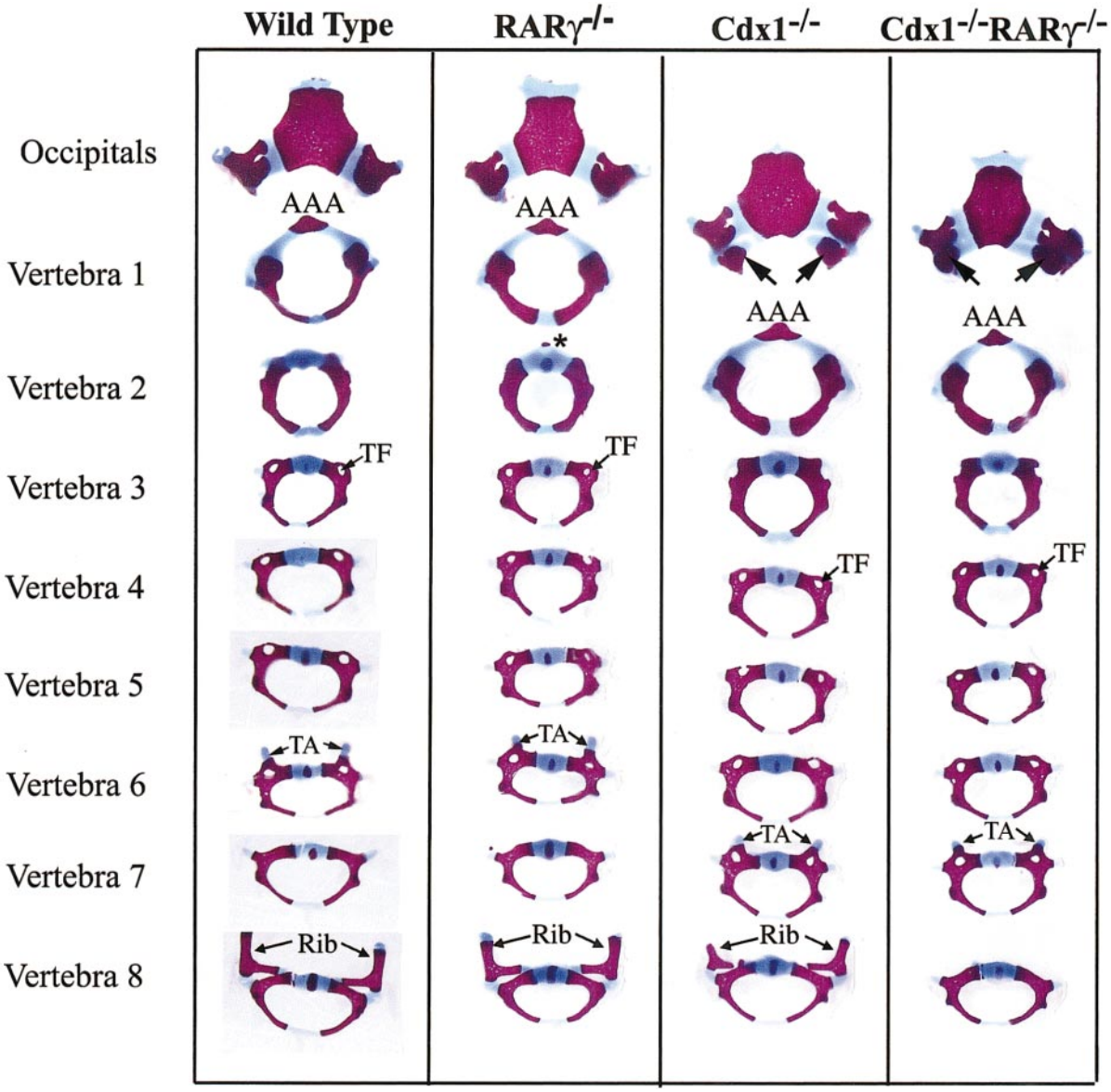

FIG. 3. Increased expressivity of vertebral defects *in Cdx1–RARγ* double null mutants. Individual vertebrae of representative skeletons from the denoted genotypes were arranged in their normal rostral–caudal sequence and photographed from an anterior perspective. The asterix on vertebra 2 of the RARγ null mutant indicates an ectopic anterior arch of the atlas. Note the increased fusion of vertebra 1 to the occipitals in the $Cdx1^{-/-}$--$RAR\gamma^{-/-}$ specimen relative to the *Cdx1* null mutant, indicated by the arrows. Note also the anterior transformation of vertebrae 2, 3, and 7 in the $Cdx1^{-/-}$ and $Cdx1^{-/-}RAR\gamma^{-/-}$ samples, evidenced by the location of the transverse foramen and the tuberculi anterior, respectively. Note also the anterior transformation of vertebra 8 to a cervical identity, indicated by the lack of ribs on this element, only in the double mutants. Abbreviations: AAA, anterior arch of the atlas; TF, transverse foramen; TA, tuberculi anterior.

C2, C3, C6, C7, and T1 (Fig. 4E, and data not shown) demonstrating that excess RA can suppress many of the vertebral defects elicited by loss of *Cdx1*. $Cdx1^{+/-}$ and $Cdx1^{-/-}$ skeletons generally exhibited posterior transformations typical of RA treatment at this stage at a comparable frequency to controls (Table 2). In this regard, however, the proatlas induced in both *Cdx1* heterozygous and null mutants was not completely formed, typically presenting as an extra pair of neural arches (Fig. 4D). Posterior transformation of C2 to a C3-like identity was also reduced (Table 2). Therefore, the incidence or severity of these RA-induced transformations depends on *Cdx1*.

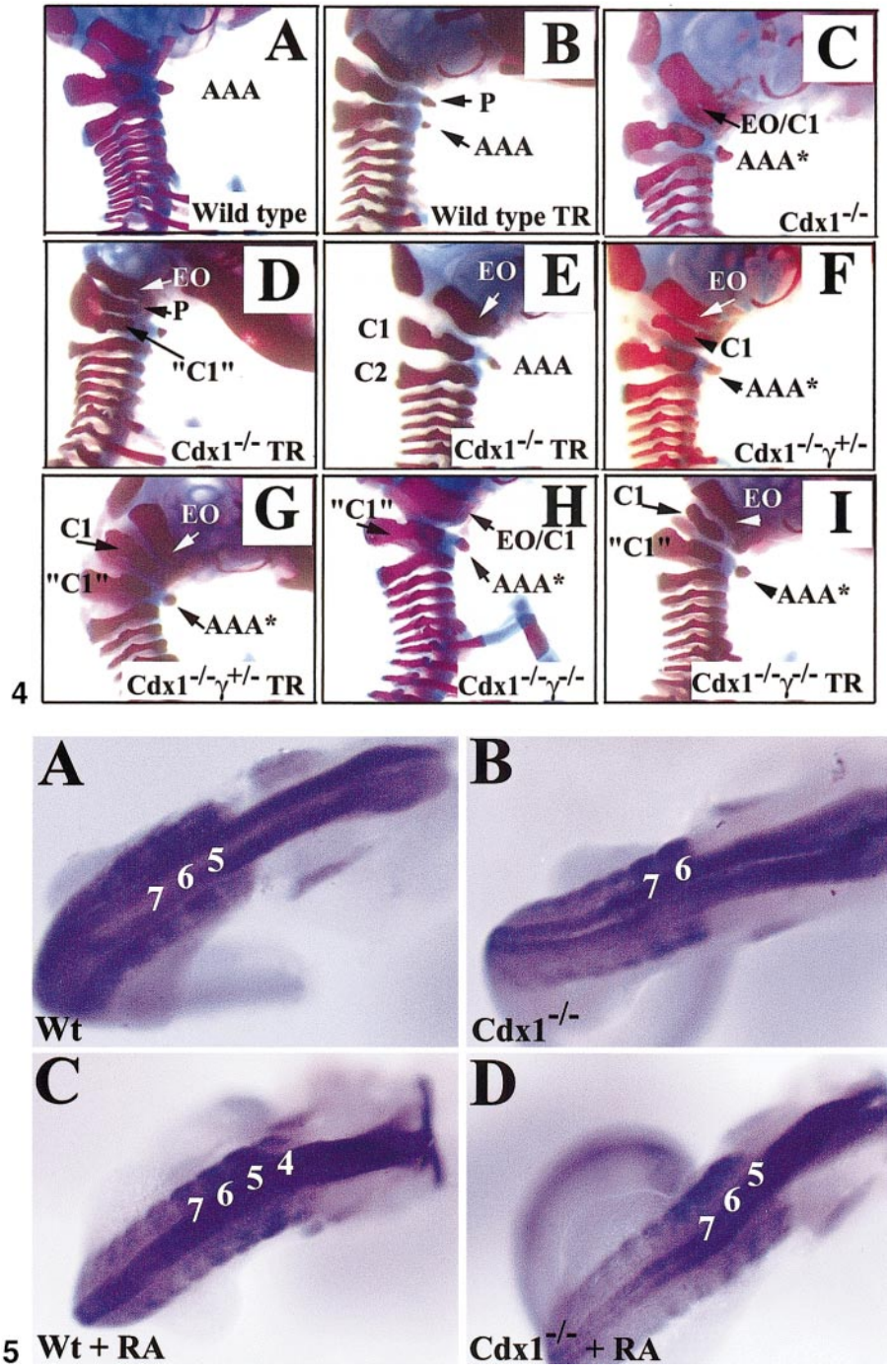

FIG. 4. The effect of exogenous RA on vertebral patterning in *Cdx1* null mutants. (A, B) Skeletal preparations from wild-type offspring without (A) or following (B) RA exposure at E7.5. Note the appearance of a proatlas following treatment (P in panel B). (C–E) *Cdx* null mutants without (C) or following (D, E) RA treatment at E7.5. Induction of a proatlas in *Cdx* null mutants was less penetrant and less expressive than in wild type samples (P in panel D vs. B). RA-treated *Cdx1* null mutants typically exhibited an essentially normal cervical skeleton, with anterior transformations and C1-exoccipital fusions no longer evident (E, compare to C and A). (F–I) Skeletal preparations of $Cdx1^{-/-}RAR\gamma^{+/-}$ (F, G) and $Cdx1^{-/-}RAR\gamma^{-/-}$ (H, I) offspring untreated (F, H) or following RA treatment at E7.5 (G, I). Note that the defects inherent to these compound mutants are only moderately ameliorated by RA treatment, as indicated by the partial fusion of C1 to the exoccipital bone and anterior transformation of C2 to C1 (arrow and AAA* respectively in F and I). Abbreviations: AAA, anterior arch of the atlas; AAA*, ectopic anterior arch of the atlas; C, cervical vertebra; "C," vertebrae with characteristics of the designated cervical vertebra; EO, exoccipital bone; EO/C1, fusions between the exoccipital bond and C1; P, proatlas.

RARγ Conveys the Effects of RA in Cdx1 Mutants

In marked contrast to *Cdx1* null mutants, almost all RA-treated *Cdx1*$^{-/-}$*RARγ*$^{+/-}$ or *Cdx1*$^{-/-}$*RARγ*$^{-/-}$ skeletons exhibited a complete C2-to-C1 anterior transformation typical of the untreated mutants (Figs. 4G and 4I; Table 2). This trend was also noted as regards C3-to-C2 anterior transformation, which was likewise unaffected by treatment. More posterior elements, however, exhibited a different response. C6-to-C5 and C7-to-C6 homeosis, which were observed in nearly all *Cdx1*$^{-/-}$, *Cdx1*$^{-/-}$*RARγ*$^{+/-}$, and *Cdx1*$^{-/-}$*RARγ*$^{-/-}$ skeletons, were attenuated completely by RA in the *Cdx1*$^{-/-}$ background and were significantly inhibited following treatment in *Cdx1*$^{-/-}$*RARγ*$^{+/-}$ and *Cdx1*$^{-/-}$*RARγ*$^{-/-}$ mutants (Table 2). Therefore, unlike the nearly complete resistance to RA-rescue of more anterior vertebrae observed in the *Cdx1*$^{-/-}$*RARγ*$^{+/-}$ and *Cdx1*$^{-/-}$*RARγ*$^{-/-}$ backgrounds, rescue of more posterior vertebrae was less dependent on RARγ, suggesting that another RAR transduces the effects of exogenous RA on these posterior elements.

All of the *Cdx1*$^{+/-}$*RARγ*$^{+/-}$, *Cdx1*$^{+/-}$*RARγ*$^{-/-}$, *Cdx1*$^{-/-}$*RARγ*$^{+/-}$, and *Cdx1*$^{-/-}$*RARγ*$^{-/-}$ offspring were also remarkably resistant to RA-induced homeotic transformations (Table 2). Induction of a proatlas and posterior transformation of C1 and C2 were never observed in the RA-treated compound *Cdx1/RARγ* mutants, and the C5-to-C6 and C6-to-C7 transformations were likewise abolished. Vertebrae C3 through C5 were never deleted and the incidence of posterior transformation of C7 to T1 was also reduced in the *Cdx1*$^{+/-}$*RARγ*$^{+/-}$ and *Cdx1*$^{+/-}$*RARγ*$^{-/-}$ backgrounds (Figs. 2G and 2I, and data not shown). Intriguingly, the incidence of many of these RA-induced defects was not significantly altered in the *RARγ* or *Cdx1* single mutants. However, the loss of one allele of each transcription factor resulted in a significant resistance to treatment. These data suggest that exogenous RA impacts on cervical vertebral patterning via convergence of both *RARγ*- and *Cdx1*-dependent pathways at E7.5.

Attenuation of the Cdx1 Null Phenotype by RA Correlates with Normalized Hox Gene Expression

Cdx1 disruption results in posteriorized *Hox* expression, while RA treatment at gastrulation generally results in anteriorized *Hox* gene expression (Subramanian *et al.*, 1995; Kessel and Gruss, 1991). In both instances, these alterations in pattern of expression correlate with vertebral homeosis. We therefore explored altered *Hox* expression as a potential molecular mechanism for RA in attenuating certain of the vertebral defects inherent to the *Cdx1* null mouse. *Hoxd3* mutants exhibit a C1-exoccipital fusion reminiscent of that seen in the *Cdx1*$^{-/-}$ background (Condie and Capecchi, 1994). Consistent with prior work (Subramanian *et al.*, 1995), we found that *Hoxd3* was posteriorized by one somite in *Cdx1* null mutants (Fig. 5B). In wild-type embryos, exogenous RA administered on E7.5 resulted in anteriorization of *Hoxd3* expression by one somite at E9.5 (Fig. 5C). RA also induced anteriorization of *Hoxd3* in *Cdx1* null littermates (Fig. 5D). However, in this case, since expression was initially posteriorized by one somite, the effect of RA was to reset the anterior limit of *Hoxd3* expression to its normal boundary. This is consistent with the rescue effect of RA on the C1-exoccipital fusion in the *Cdx1* null background being mediated, in part, by altered *Hoxd3* expression. Whether similar effects on other *Hox* genes are involved in this or other RA-induced outcomes in the *Cdx1* mutant background is presently under investigation.

DISCUSSION

We previously demonstrated that *Cdx1* is an RAR target gene, suggesting an indirect means by which RA could affect vertebral patterning (Houle *et al.*, 2000). To further assess the relationship between retinoid signaling and *Cdx1*, we generated and analyzed *Cdx1–RARγ* compound null mutants. Our present data clearly demonstrate a synergistic relationship between these transcription factors, with *RARγ-Cdx1* double heterozygotes exhibiting defects that are not observed at a high frequency in either single heterozygote background. Moreover, the effects of RA on vertebral patterning are partially mitigated in the absence of Cdx1. These findings are consistent with RA functioning upstream of *Cdx1* in vertebral patterning along the A-P axis. However, *Cdx1–RARγ* double mutants were more affected than either single null mutant, and exogenous RA impacted on vertebral patterning and *Hox* expression in *Cdx1* null offspring. These observations demonstrate that retinoid signaling also affects vertebral patterning through means other than (or in addition to) regulation of *Cdx1*.

Cdx1 and RARγ Act Synergistically in Vertebral Patterning

The significant increase in penetrance and expressivity of the cervical transformations in *Cdx1–RARγ* double het-

FIG. 5. Cdx1 and exogenous RA converge on expression of *Hoxd3* in the mesoderm. *Hoxd3* expression was assessed by whole-mount *in situ* hybridization in E9.5 embryos either untreated (A, B) or after exposure to RA at E7.5 (C, D). (A) *Hoxd3* expression in an untreated wild-type control, exhibiting the anterior limit of expression in somite 5 typical of *Hoxd3*. (B) An untreated *Cdx1* null mutant exhibiting posteriorized expression in somite 6. RA treatment anteriorized expression in both wild-type (C) and *Cdx1* null mutants (D) by one somite, to somite 4 or 5, respectively.

erozygotes, relative to either single heterozygote, demonstrates that these transcription factors act synergistically to specify vertebral identity. There are several potential mechanisms by which this could occur. First, RARγ and Cdx1 may converge on a common target gene(s), with both factors contributing to transcription. In this regard, a putative Cdx binding site has been identified in close proximity to an RARE in the 3′ region of the *Hoxd4* gene (Zhang *et al.*, 2000). However, *Hoxd4* expression is not detectably affected in *RARγ* mutants (Folberg *et al.*, 1999) or *RARγ–Cdx1* double null offspring (data not shown).

A second possibility is that RARγ and Cdx1 regulate the expression of distinct, separate, target genes which converge on vertebral patterning in a synergistic manner. In this regard, RA is unable to rescue the C2-to-C1 transformation seen in *Hoxd4* mutants (Folberg *et al.*, 1999), although it does so in RARγ null offspring (Iulianella and Lohnes, 1997). This suggests that *Hoxd4* and retinoid signaling regulate parallel but distinct pathways which converge on C2 morphogenesis. Given the interactions between *Hox* paralog group 4 genes in patterning this element, these paralogs are a logical target. In this regard, however, we have not observed altered *Hoxb4* expression in *Cdx1–RARγ* double null embryos, although subtle differences may be below the limit of detection of *in situ* hybridization.

As a final mechanism for synergy, *Cdx1* may be further reduced in the compound mutants by virtue of decreased RA-dependent expression of *Cdx1* (Houle *et al.*, 2000). In this regard, however, we have not noted significant loss of *Cdx1* expression in the RARγ null backgound (our unpublished observations), although subtle differences cannot be excluded. *Cdx1* autoregulation (P. Panagiotis *et al.*, in press] may also contribute to decreased *Cdx1* expression in these mutant backgrounds with attendant phenotypic consequences. Consistent with either of the above mechanisms, we have found that *Cdx1* heterozygotes exhibit a phenotype, and therefore small alterations in Cdx1 levels would be anticipated to have phenotypic consequences. In any event, as the *Cdx1-RARγ* double null mutant phenotype is more severe than either single null mutant, retinoid-dependent vertebral specification must occur through other processes, in addition to regulation of *Cdx1* expression.

Analysis of this allelic series revealed that compound mutants (e.g., RARγ$^{-/-}$/Cdx1$^{+/-}$ offspring) exhibited vertebral malformations such as dorsal fusions of the neural arches not typically classed as homeotic transformations. However, subsequent removal of (in this example) the remaining *Cdx1* allele resulted in double null mutants with a remarkably normal cervical skeleton (although anteriorized by one vertebra). This observation suggests that these vertebral fusions, which are also characteristic of a number of *Hox* and RAR mutants, are indicative of an intermediate degree of homeosis which becomes fully resolved in the double null mutants. Moreover, alterations in gene expression would be anticipated to be quite subtle, since loss of two or more *Hox* genes usually results in large regional homeosis (e.g., Horan *et al.*, 1995a,b) or deletion of entire vertebrae (e.g., Condie and Capecchi, 1994). Such malformations were not observed here, suggesting that loss of *RARγ* and *Cdx1* results in a repatterning of vertebral identities in a restricted manner. Indeed, all *Hox* genes previously examined in the *Cdx1* null mutants are shifted by only one somite, with the exception of *Hoxc5* which is posteriorized by two somites (Subramanian *et al.*, 1995).

Cdx1 and RA in Vertebral Specification.

Cdx1 misexpression can lead to neural tube and vertebral defects in both mouse and in *Xenopus* (Charité *et al.*, 1998; Isaacs *et al.*, 1998; Pownall *et al.*, 1996). RA treatment at E7.5–E8.5 results in a large increase in *Cdx1* expression in the primitive streak region, while exposure at E9.5–E10.5 induces expression in the limb buds (Houle *et al.*, 2000); development of each of these structures is profoundly affected by retinoid excess at these stages (Ross *et al.*, 2000). These observations raised the possiblity that *Cdx1* may mediate certain retinoid-induced teratogenic outcomes. However, offspring from *Cdx1*$^{+/-}$ intercrosses exposed to a teratogenic bolus of RA at E7.5–E10.5 exhibited identical frequencies and severity of caudal truncation or limb defects irrespective of genotype. Therefore, *Cdx1* appears to be dispensable as regards the etiology of these particular teratogenic outcomes. The lack of a critical role for *Cdx1* in retinoid-induced axial truncation is consistent with our finding that it is induced by RA in RARγ null mutant embryos, yet this receptor is essential for mediating this particular teratogenic outcome (Lohnes *et al.*, 1993).

The phenotype of *Cdx1* null mice is limited essentially to the rostral vertebral column. RA excess or RAR disruption has strong effects on both vertebral patterning as well as *Cdx1* expression at E7.5, the window during which the occipital and cervical somites are presumably patterned. These observations suggested that *Cdx1* may mediate the effects of RA on the cervical skeleton. To assess this, we compared vertebral patterning between wild type and *Cdx1* null offspring following treatment with vehicle or RA at E7.5. This analysis indicated that *Cdx1* null mutants were partially resistant to the formation of a proatlas as well as posterior transformation of C1 or C2 evoked by RA treatment at this stage. Although this is a pharmacological setting, this observation offers further support for *Cdx1* as a retinoid target involved in patterning the rostral vertebral column.

Cdx1 Is Not the Sole Player in RA-Dependent Vertebral Patterning

Our present data demonstrate that *Cdx1* interacts synergistically with RARγ and contributes to some of the posteriorizing effects of excess RA at E7.5. These observations are consistent with a role for this transcription factor as a retinoid target gene involved in vertebral patterning. However, the significant increase in penetrance of the T1-to-C7

and L1-to-thoracic anterior transformations and the increased expressivity of the C1–occipital fusions in *Cdx1–RARγ* double mutants, relative to single null offspring, demonstrates that RARγ must regulate the expression of other factors involved in specification of these elements in addition to *Cdx1*. This observation also demonstrates a role for RARγ in patterning the anterior cervical and posterior thoracic vertebrae, a function that is masked in the presence of *Cdx1*.

Further evidence that RARγ regulates target genes involved in vertebral patterning distinct from *Cdx1* is provided by the observation that the vertebrae of *Cdx1* null mutants are sensitive to exogenous RA, and these effects are largely attenuated by subsequent disruption of *RARγ*. For example, relative to wild-type offspring, the induction of a proatlas is marginally attenuated in RA-treated *Cdx1* or *RARγ* null mutants but it is never induced in *Cdx1-RARγ* mutants. RA-treatment of *Cdx1* null embryos at E7.5 also results in a rescue of certain of the vertebral transformations inherent to this mutant background. Again, these effects are mediated at least in part by RARγ, as such rescue is greatly reduced in the double null mutant background. In this regard, it is interesting to note that disruption of only a single copy of *RARγ* suffices to suppress many of the effects of RA in the *Cdx1* null mutant background, while only minimal changes in retinoid-response are seen in *RARγ* heterozygotes (relative to wild type). This strong gene dose-dependency is consistent with these signaling pathways converging on common targets.

As discussed above, convergence of these pathways could conceivably occur by regulation of a common target gene. Alternatively, RA and *Cdx1* may regulate different target genes that both influence a common event. In the latter case, several *Hox* gene products have been shown to mediate highly similar functions as pertains to vertebral patterning (Horan *et al.*, 1995a,b; Condie and Capecchi, 1994; Greer *et al.*, 2000). In this regard, *Hoxd3* is posteriorized by one somite in *Cdx1* null embryos at E9.5, and the phenotype of *Hoxd3* null mutants is markedly similar to *Cdx1* mutants with respect to fusion of C1 and the occipitals (Subramanian *et al.*, 1995). One of the most striking effects of RA in *Cdx1* mutants is the restoration of a relatively normal cervical region, including C1. These observations suggest that *Hoxd3* may represent a common target for these pathways. Consistent with this, we found that RA treatment of both wild-type and *Cdx1* null mutant embryos at E7.5 anteriorized *Hoxd3* expression by one somite. However, as *Hoxd3* is posteriorized by one somite in untreated *Cdx1* mutants, this treatment resulted in reestablishment of the normal anterior boundary of expression concomitant with rescue of C1 morphology. These data clearly demonstrate that RA can affect mesodermal *Hox* expression in the absence of Cdx1. Moreover, these results also suggest that exogenous RA attenuates some aspects of the *Cdx1* null phenotype via convergent effects on regulation of *Hoxd3* expression. However, it should be noted that, in *Hoxd3* null mutants, reduced neural arches of C1 persist, while they are largely absent in *Cdx1* null skeletons. This implies that additional *Hox* genes involved in patterning of C1 are affected by *Cdx1* disruption. In this regard, *Hoxa3/Hoxd3* and *Hoxb3/Hoxd3* double mutants display a more complete C1–occipital fusion accompanied by the loss of C1 neural arches (Manley and Capecchi, 1997). Together with the finding that RA treatment at E7.5 anteriorizes the mesodermal expression of *Hoxa3* (Kessel and Gruss, 1991), it is likely that Cdx1 and RA converge on several *Hox* group 3 genes involved in patterning the rostral axial skeleton. The identity of the *Hox* genes involved in mediating the other effects of RA in the *Cdx1* null background is presently under investigation.

ACKNOWLEDGMENTS

We thank Mark Featherstone and Mario Cappechi for probes used in this study, and members of the group for their comments. This work was supported by grants from the Canadian Institutes for Health Research and the March of Dimes Birth Defects Foundation (#1-FY00-694) to D.L. D.A. was supported by a scholarship from the Natural Sciences and Engineering Council of Canada and a Lloyd Carr–Harris McGill Major Fellowship. M.H. was supported by a scholarship from the Canadian Institutes for Health Research. D.L. is a chercheur boursier (Junior 2) of the Fonds de la Recherches en Santé de Québec.

REFERENCES

Beck, F., Erler, T., Russell, A., and James, R. (1995). Expression of cdx2 in the mouse embryo and placenta: Possible role in patterning of the extra-embryonic membranes. *Dev. Dyn.* **204,** 219–227.

Beddington, R. S., and Robertson, E. J. (1999). Axis development and early asymmetry in mammals. *Cell* **96,** 195–209.

Burke, A. C., Nelson, C. E., Morgan, B. A., and Tabin C. (1995). Hox genes and the evolution of vertebrate axial morphology. *Development* **121,** 333–346.

Capecchi, M. R. (1997). Hox genes and mammalian development. *Cold Spring Harbor Symp. Quant. Biol.* **62,** 273–281.

Chambon, P. (1996). A decade of molecular biology of retinoic acid receptors. *FASEB J.* **10,** 940–954.

Charité, J., de Graaff, W., Consten, D., Reijnen, M. J., Korving, J., and Deschamps, J. (1998). Transducing positional information to the Hox genes: Critical interaction of cdx gene products with position-sensitive regulatory elements. *Development* **125,** 4349–4358.

Chawengsaksophak, K., James, R., Hammond, V. E., Kontgen, F., and Beck, R. (1997). Homeosis and intestinal tumours in Cdx2 mutant mice. *Nature* **386,** 84–87.

Christ, B., Huang, R., and Wilting J. (2000). The development of the avian vertebral column. *Anat. Embryol.* **202,** 179–194.

Condie, B. G., and Capecchi, M. R. (1993). Mice homozygous for a targeted disruption of Hoxd-3 (Hox4.1) exhibit anterior transformations of the first and second cervical vertebrae, the atlas and the axis. *Development* **119,** 579–595.

Condie, B. G., and Capecchi M.R. (1994). Mice with targeted disruptions in the paralogous genes Hoxa-3 and Hoxd-3 reveal synergistic interactions. *Nature* **370,** 304–307.

Conlon, R. A. (1995). Retinoic acid and pattern formation in vertebrates. *Trends Genet.* **11,** 314–319.

Conlon, R. A., and Rossant, J. (1992). Exogenous retinoic acid rapidly induces anterior ectopic expression of murine Hox2 genes in vivo. *Development* **116,** 357–368.

Dupé, V., Davenne, M., Brocard, J., Dollé, P., Mark, M., Dierich, A., Chambon, P., and Rijli, F. M. (1997). In vivo functional analysis of the Hoxa-1 3′ retinoic acid response element (3′RARE). *Development* **124**, 399–410.

Favier, B., and Dollé, P. (1999). Developmental functions of mammalian Hox genes. *Mol. Hum. Reprod.* **3,** 115–131.

Folberg, A., Kovacs, E. N., and Featherstone, M. S. (1997). Characterization and retinoic acid responsiveness of the murine Hoxd-4 transcription unit. *J. Biol. Chem.* **272,** 29151–29157.

Folberg, A., Nagy-Kovács, E., Lohnes, D., and Featherstone, M. S. (1999). Hoxd-4 and Rarγ interact synergistically in the specification of the cervical vertebrae. *Mech. Dev.* **89,** 65–74.

Frasch, M., Chen, X., and Lufkin, T. (1995). Evolutionary-conserved enhancers direct region-specific expression of the murine Hoxa-1 and Hoxa-2 loci in both mice and drosophila. *Development* **121,** 957–974.

Gale, E., Zile, M., and Maden, M. (1999). Hindbrain respecification in the retinoid-deficient quail. *Mech. Dev.* **89,** 43–54.

Gamer, L. W., and Wright, C. V. (1993). Murine cdx4 bears striking similarities to the drosophila caudal gene in its homeodomain sequence and early expression pattern. *Mech. Dev.* **43,** 71–81.

Gaunt, S. J. (1994). Conservation in the Hox code during morphological evolution. *Int. J. Dev. Biol.* **38,** 549–552.

Greer, J. M., Puetz, J., Thomas, K. R., and Capecchi, M. R. (2000). Maintenance of functional equivalence during paralogous Hox gene evolution. *Nature* **403,** 661–665.

Gruss, P., and Kessel, M. (1991). Axial specification in higher vertebrates. *Curr. Opin. Genet. Dev.* **1,** 204–210.

Horan, G. S., Kovacs, E. N., Behringer, R. R., and Featherstone, M. S. (1995a). Mutations in paralogous Hox genes result in overlapping homeotic transformations of the axial skeleton: Evidence for unique and redundant function. *Dev. Biol.* **169** 359–372.

Horan, G. S., Ramirez-Solis, R., Featherstone, M. S., Wolgemuth, D. J., Bradley, A., and Behringer, R. R. (1995b). Compound mutants for the paralogous Hoxa-4, Hoxb-4, and Hoxd-4 genes show more complete homeotic transformations and a dose-dependent increase in the number of vertebrae transformed. *Genes Dev.* **9,** 1667–1677.

Houle, M., Prinos, P., Iulianella, A., Bouchard N., and Lohnes, D. (2000). Cdx1 is a direct retinoic acid receptor target gene; a new pathway for retinoids and vertebral specification. *Mol. Cell. Biol.* **20,** 6579–6586.

Huang, D., Chen, S. W., Langston, A. W., and Gudas, L. J. (1998). A conserved retinoic acid responsive element in the murine Hoxb-1 gene is required for expression in the developing gut. *Development* **125,** 3235–3246.

Isaacs, H. V., Pownall, M. E., and Slack, J. M. (1998). Regulation of Hox gene expression and posterior development by the Xenopus caudal homologue Xcad3. *EMBO J.* **17,** 3413–3427.

Iulianella, A., Folberg, A., Petkovich, M., and Lohnes, D. (1999). A molecular basis for retinoic acid-induced axial truncation. *Dev. Biol.* **205,** 33–48.

Iulianella, A., and Lohnes, D. (1997). Contribution of retinoic acid receptor gamma to retinoid-induced craniofacial and axial defects. *Dev. Dyn.* **209,** 92–104.

Kastner, P., Mark, M., and Chambon P. (1996). Nonsteroid nuclear receptors: What are genetic studies telling us about their role in real life? *Cell* **83,** 859–869.

Kessel, M., and Gruss, P. (1991). Homeotic transformations of murine vertebrae and concomitant alteration of Hox codes induced by retinoic acid. *Cell* **67,** 89–104.

Langston, A. W., and Gudas, L. J. (1992). Identification of a retinoic acid responsive enhancer 3′ of the murine homeobox gene Hox1.6. *Mech. Dev.* **38,** 217–227.

Lohnes, D., Kastner, P., Dierich, A., Mark, M., LeMeur, M., and Chambon,. P. (1993). Function of retinoic acid receptor gamma in the mouse. *Cell* **73,** 643–658.

Lohnes, D., Mark, M., Mendelsohn, C., Dollé, P., Dierich, A., Gorry, P., Gansmuller, A., and Chambon, P. (1994). Function of the retinoic acid receptors (RARs) during development. (I) Craniofacial and skeletal abnormalities in RAR double mutants. *Development* **120,** 2723–2748.

Maconochie, M., Nonchev, S., Morrison, A., and Krumlauf, R. (1996). Paralogous Hox genes function and regulation. *Annu. Rev. Genet.* **30,** 529–556.

Maden, M., Gale, E., Kostetskii, I., and Zile, M. (1996). Vitamin A-deficient quail embryos have half a hindbrain and other neural defects. *Curr. Biol.* **6,** 417–426.

Maden, M., Graham, A., Zile, M., and Gale, E. (2000). Abnormalities of somite development in the absence of retinoic acid. *Int. J. Dev. Biol.* **44,** 151–159.

Mangelsdorf, D. J., Thummel, C., Beato, M., Herrlich, P., Schultz, G., Umesono, K., Blumberg, B., Kastner, P., Mark, M., Chambon, P., and Evans R. M. (1996). The nuclear receptor superfamily: The second decade. *Cell* **83,** 835–839.

Manley, N. R., and Capecchi, M. R. (1997). Hox group 3 paralogous genes act synergistically in the formation of somitic and neural crest-derived structures. *Dev. Biol.* **192,** 274–288.

Marshall, H., Nonchev, S., Sham, M. H., Muchamore, I., Lumsden, A., and Krumlauf. R. (1992). Retinoic acid alters hindbrain Hox code and induces transformation of rhombomeres 2/3 into a 4/5 identity. *Nature* **360,** 737–741.

Marshall, H., Studer, M., Pöpperl, H., Aparicio, S., Kuroiwa, A., Brenner, S., and Krumlauf, R. (1994). A conserved retinoic acid response element required for early expression of the homeobox gene Hoxb-1. *Nature* **370,** 567–571.

Marshall, H., Morrison, A., Studer, M., Popperl, H., and Krumlauf, R. (1996). Retinoids and Hox genes. *FASEB J.* **10,** 969–978.

Meyer, B. I., and Gruss, P. (1993). Mouse Cdx1 expression during gastrulation. *Development* **117,** 191–203.

Morrison, A., Moroni, M. C., Ariza-McNaughton, L., Krumlauf, R., and Mavilio, F. (1996). In vitro and transgenic analysis of a human Hoxd4 retinoid-responsive enhancer. *Development* **122**, 1895–1907.

Niederreither, K., Subbarayan, V., Dolle, P., and Chambon, P. (1999). Embryonic retinoic acid synthesis is essential for early mouse post-implantation development. *Nat. Genet.* **21**, 444–448.

Niederreither, K., Vermot, J., Schuhbaur, B., Chambon, P., and Dollé. P. (2000). Retinoic acid synthesis and hindbrain patterning in the mouse embryo. *Development* **127,** 75–85.

Oh, S. P., and Li, E. (1997). The signaling pathway mediated by the type IIB activin receptor controls axial patterning and lateral asymmetry in the mouse. *Genes Dev.* **11,** 1812–1826.

Packer, A. I., Crotty, D. A., Elwell, V. A., and Wolgemuth, D. J. (1998). Expression of the murine Hoxa4 gene requires both

autoregulation and a conserved retinoic acid response element. *Development* **125,** 1991–1998.

Partanen, J., Schwartz, L., and Rossant, J. (1998). Opposite phenotypes of hypomorphic and y766 phosphorylation site mutations reveal a function for fgfr1 in anteroposterior patterning of mouse embryos. *Genes Dev*. **12,** 2332–2344.

Pöpperl, H., and Featherstone, M. S. (1993). Identification of a retinoic acid response element upstream of the murine Hox4.2 gene. *Mol. Cell. Biol*. **13,** 257–265.

Pownall, M. E., Tucker, A. S., Slack, J. M., and Isaacs, H. V. (1996). eFGF, Xcad3 and Hox genes form a molecular pathway that establishes the anteroposterior axis in Xenopus. *Development* **122,** 3881–3892.

Prinos, P., Joseph, S., Oh, K., Meyer, B., Gruss, P., and Lohnes, D. (2001). Multiple pathways govern Cdx1 expression during murine development., doi:10.1006/dbio.2001.0446.

Ross, S. A., McCaffery, P. J., Drager, U. C., and De Luca, L. M. (2000). Retinoids in embryonal development. *Physiol. Rev*. **80,** 1021–1054.

Sharkey, M., Graba, Y., and Scott, M. P. (1997). Hox genes in evolution: Protein surfaces and paralog groups. *Trends Genet*. **13,** 145–151.

Simeone, A., Acampora, D., Arcioni, L., Andrews, P. W., Boncinelli, E., and Mavilio, F. (1990). Sequential activation of Hox2 homeobox genes by retinoic acid in human embryonal carcinoma cells. *Nature* **346,** 763–766.

Studer, M., Pöpperl, H., Marshall, H., Kuroiwa, A., and Krumlauf, R. (1994). Role of a conserved retinoic acid response element in rhombomere restriction of Hoxb-1. *Science* **265,** 1728–1732.

Subramanian, V., Meyer, B. I., and Gruss, P. (1995). Disruption of the murine homeobox gene cdx1 affects axial skeletal identities by altering the mesodermal expression domains of Hox genes. *Cell* **83,** 641–653.

Wilson, V., and Beddington, R. S. (1996). Cell fate and morphogenetic movement in the late mouse primitive streak. *Mech. Dev*. **55,** 79–89.

Yu, B. D., Hess, J. L., Horning, S. E., Brown, G. A., and Korsmeyer, S. J. (1995). Altered Hox expression and segmental identity in Mll-mutant mice. *Nature* **378,** 505–508.

Zhang, F., Nagy Kovacs, E., and Featherstone, M. S. (2000). Murine hoxd4 expression in the CNS requires multiple elements including a retinoic acid response element. *Mech. Dev*. **96,** 79–89.

Received for publication June 25, 2001
Revised July 25, 2001
Accepted July 27, 2001
Published online October 25, 2001